Size and shape effects on the order–disorder phase transition in CoPt nanoparticles

D. Alloyeau[1,2]*[†], C. Ricolleau[1], C. Mottet[3], T. Oikawa[1,4], C. Langlois[1], Y. Le Bouar[2], N. Braidy[1,2] and A. Loiseau[2]

Chemically ordered bimetallic nanoparticles are promising candidates for magnetic-storage applications. However, the use of sub-10 nm nanomagnets requires further study of possible size effects on their physical properties. Here, the effects of size and morphology on the order–disorder phase transition temperature of CoPt nanoparticles (T_C^{NP}) have been investigated experimentally, using transmission electron microscopy, and theoretically, with canonical Monte Carlo simulations. For 2.4–3-nm particles, T_C^{NP} is found to be 325–175 °C lower than the bulk material transition temperature, consistent with our Monte Carlo simulations. Furthermore, we establish that T_C^{NP} is also sensitive to the shape of the nanoparticles, because only one dimension of the particle (that is, in-plane size or thickness) smaller than 3 nm is sufficient to induce a considerable depression of T_C^{NP}. This work emphasizes the necessity of taking into account the three-dimensional morphology of nano-objects to understand and control their structural properties.

Permanent nanomagnets with a size below 10 nm are at the centre of intensive research for their use as ultrahigh-density magnetic-storage devices[1–3]. The main physical limitation of such a technology originates from the superparamagnetic behaviour of very small nanoparticles, as the magnetization direction reversal induced by thermal fluctuations is incompatible with long-time recording[4]. The thermal stability of the magnetization can be evaluated by comparing the thermal energy, $k_B T$, with the energy barrier, $K_u V$ (where k_B is the Boltzmann constant, T is the temperature in Kelvin, K_u is the magnetocrystalline anisotropy constant and V is the volume of the magnetic domain). For applications, the thermal stability of the magnetization requires that $(K_u V / k_B T) \geq 60$ (refs 3, 5). One of the most promising routes to maintain the thermal stability of the nanoparticles' magnetization is to use bimetallic alloys composed of $3d$ magnetic elements and $5d$ (or $4d$) elements, such as CoPt, FePt, FePd, CoRh and so on. These materials have a K_u one order of magnitude larger than CoCr-based alloys used in magnetic devices[6–8]. The highest K_u value of these alloys is obtained with a chemically ordered structure ($L1_0$) close to the equiatomic composition and below the order–disorder transition temperature (T_C^{Bulk}). Above T_C^{Bulk}, these alloys are chemically disordered on the face-centred-cubic (fcc) lattice. In these systems, the largest coercivity is concomitant with nanoparticles having the highest long-range order[9–11] (LRO). From an industrial and fundamental point of view, it is then essential to quantitatively study the relationship between the ordered state and the size of the nanoparticles.

In the past ten years, the structure and chemical ordering of such bimetallic nanoparticles have motivated numerous experimental and theoretical studies. However, only a few papers have reported experimental evidence of the size effects on the order state

occurring in Cu_3Au (ref. 12), FePt (refs 13, 14) and FePd (ref. 15) nanoparticles. In all of them, the range of sizes in which the ordered phase is inhibited by the nanoparticle dimensions is determined from transmission electron microscope (TEM) images of the nanoparticles, which are inherently a projection of the nanoparticle shape, and no attention has been devoted to the influence of their morphology. From a theoretical point of view, several groups have already reported such size effects in FePt (refs 16–18) and CoPt (refs 19, 20) nanoparticles, but a spherical geometry is commonly assumed without considering the nanoparticle morphology. The inhibition of the ordered phase is attributed to a decrease of the phase transition temperature (T_C^{NP}) when the particle size is below a few nanometres, although this explanation has never been clearly demonstrated experimentally.

Here, we investigate the influence of size and morphology on the order–disorder phase transition temperature in CoPt nanoparticles, both experimentally and theoretically. We show that this transition temperature is reduced by at least 175 °C with respect to the bulk value ($T_C^{Bulk} = 825$ °C; ref. 21) and that this size effect occurs in the presence of nanoparticles having at least one of the characteristic dimensions smaller than 3 nm (that is, either the nanoparticle diameter in the substrate plane or the nanoparticle thickness). This is achieved using a suite of quantitative electron microscopy methods including tomography, nanobeam diffraction and high-resolution imaging. The magnitude of the experimentally measured depression of the order–disorder transition temperature is moreover consistent with our theoretical calculations based on Monte Carlo simulations carried out using tight-binding interatomic potentials in the second-moment approximation. More generally, this study opens the 'conceptual' possibility to design nanoarchitectures (pillars, ellipsoids and spheres), where a different shape can change the physical properties of the materials and

[1]Laboratoire Matériaux et Phénomènes Quantiques, Université Paris 7/CNRS, Bâtiment Condorcet, 4 rue Elsa Morante, 75205 Paris Cedex 13, France, [2]Laboratoire d'Etude des Microstructures—ONERA/CNRS, B.P. 72, 92322 Châtillon, France, [3]Centre Interdisciplinaire de Nanosciences de Marseille, CNRS, Campus de Luminy, Case 913, 13288 Marseille Cedex 9, France, [4]JEOL Ltd, 1-2 Musashino 3-Chome, Akishima, Tokyo 196-8558, Japan. *Present address : Lawrence Berkeley National Laboratory (LBNL), National Center for Electron Microscopy (NCEM), 1 Cyclotron Road-MS, 72 Berkeley, California 94720, USA. [†]e-mail: alloyeau.damien@gmail.com.
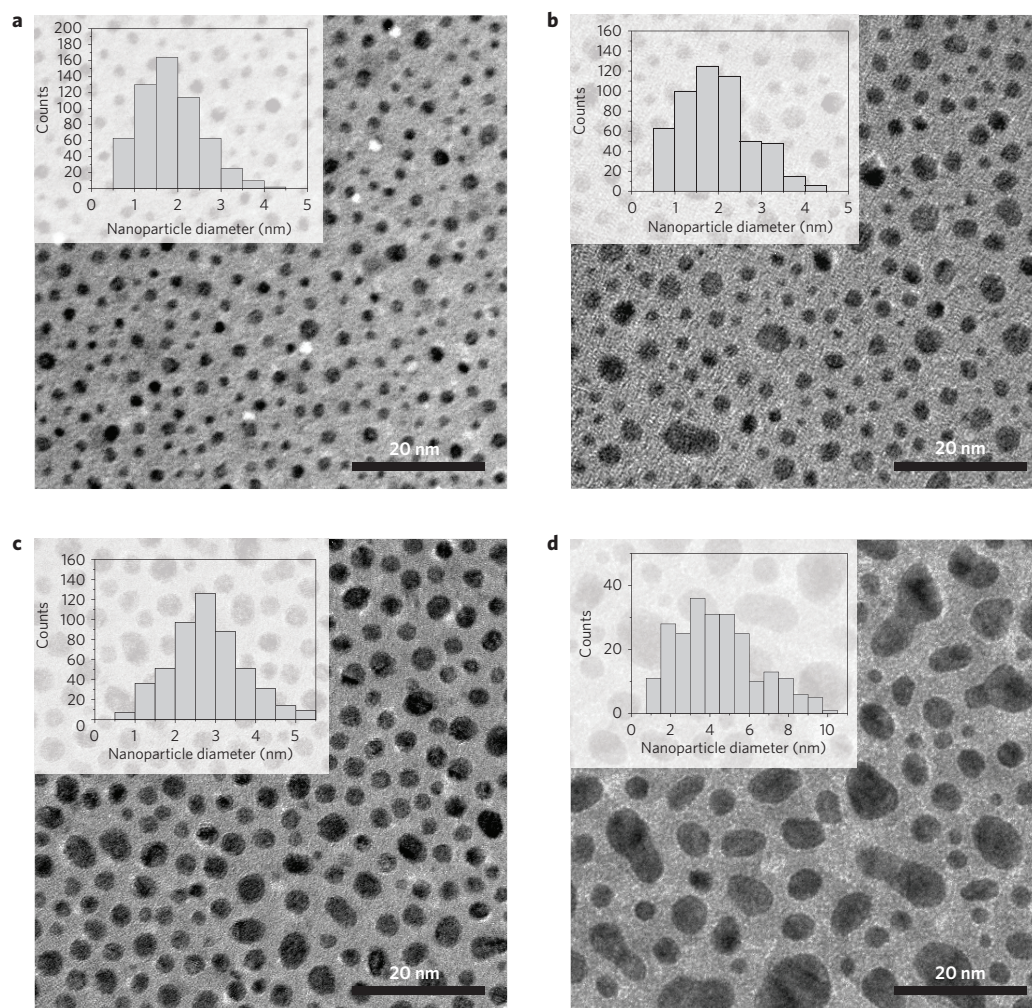
Figure 1 | Morphology of the particles projected in the substrate plane. a–d, TEM bright-field micrographs of the samples obtained with 0.5 nm (**a,b**) and 1 nm (**c,d**) nominal thicknesses annealed for 1 h at 650 °C (**a,c**) and 750 °C (**b,d**), respectively.

Table 1 | Evolution of the nanoparticle mean size and polydispersity at annealing temperatures of 650 and 750 °C for samples with a 0.5 nm and 1 nm nominal thickness (NT).

NT		As-grown	650 °C	750 °C
0.5 nm	Mean size	2 nm	2 nm	2.4 nm
	Polydispersity	30%	32%	40%
1 nm	Mean size	3 nm	3 nm	4.8 nm
	Polydispersity	33%	34%	45%

allow a better performance (for example, higher density storage for nanopillars than for flat nanoparticles).

To study the size effects on the order–disorder phenomena, we have investigated the chemical ordering of as-grown disordered $Co_{50}Pt_{50}$ nanoparticles prepared by pulsed laser deposition (PLD; see the Methods section). As-grown nanoparticles on a substrate held at a temperature lower than 600 °C are chemically disordered, and the ordering of CoPt nanoparticles is routinely induced following an annealing step above 600 °C to activate atomic diffusion within the particles[22–24] but under 800 °C to avoid the order–disorder transition. Disordered CoPt nanoparticles have been fabricated on amorphous carbon films supported on a Cu TEM grid at room temperature with a 0.5 and 1 nm nominal thickness. The bimetallic nanoparticles were randomly oriented on

the amorphous carbon substrate, and neither texture nor epitaxy was detected. The mean size of the as-grown nanoparticles of each sample was respectively 2 and 3 nm (Table 1). The particles were then covered with a 2-nm-thick protective layer of amorphous alumina. The samples were finally annealed at 650 and 750 °C for 1 h. The results are based on the analysis of six samples, as indicated in Table 1: two as-grown samples, to analyse the morphology of the nanoparticles before the annealing (pictures not shown), two samples annealed at 650 °C (with a nominal thickness of 0.5 and 1 nm) and two samples annealed at 750 °C (with a nominal thickness of 0.5 and 1 nm). The nanoparticle composition before and after the annealing step was determined by energy-dispersive X-ray analysis carried out on a nanoparticle assembly (TEM mode) and on single nanoparticles (scanning transmission electron microscopy (STEM) mode). The X-ray analyser was calibrated by determining the Cliff–Lorimer k factor ratio between Co and Pt on a bulk $Co_{45}Pt_{55}$ sample (see the Methods section). The composition of the nanoparticle assemblies before and after annealing is $Co_{50}Pt_{50}$ (±3%). Similarly, the composition of single nanoparticles in the range of size from 1.5 to 6 nm was found to be $Co_{50}Pt_{50}$ with a dispersion of ±8%, which is larger than for nanoparticle assemblies because of the lower X-ray count statistics.

Figure 1 shows one representative TEM bright-field micrograph of each specimen following annealing at 650 and 750 °C. During annealing, the mean size, the polydispersity (that is, standard deviation divided by the mean size) (Table 1) and the size distribution
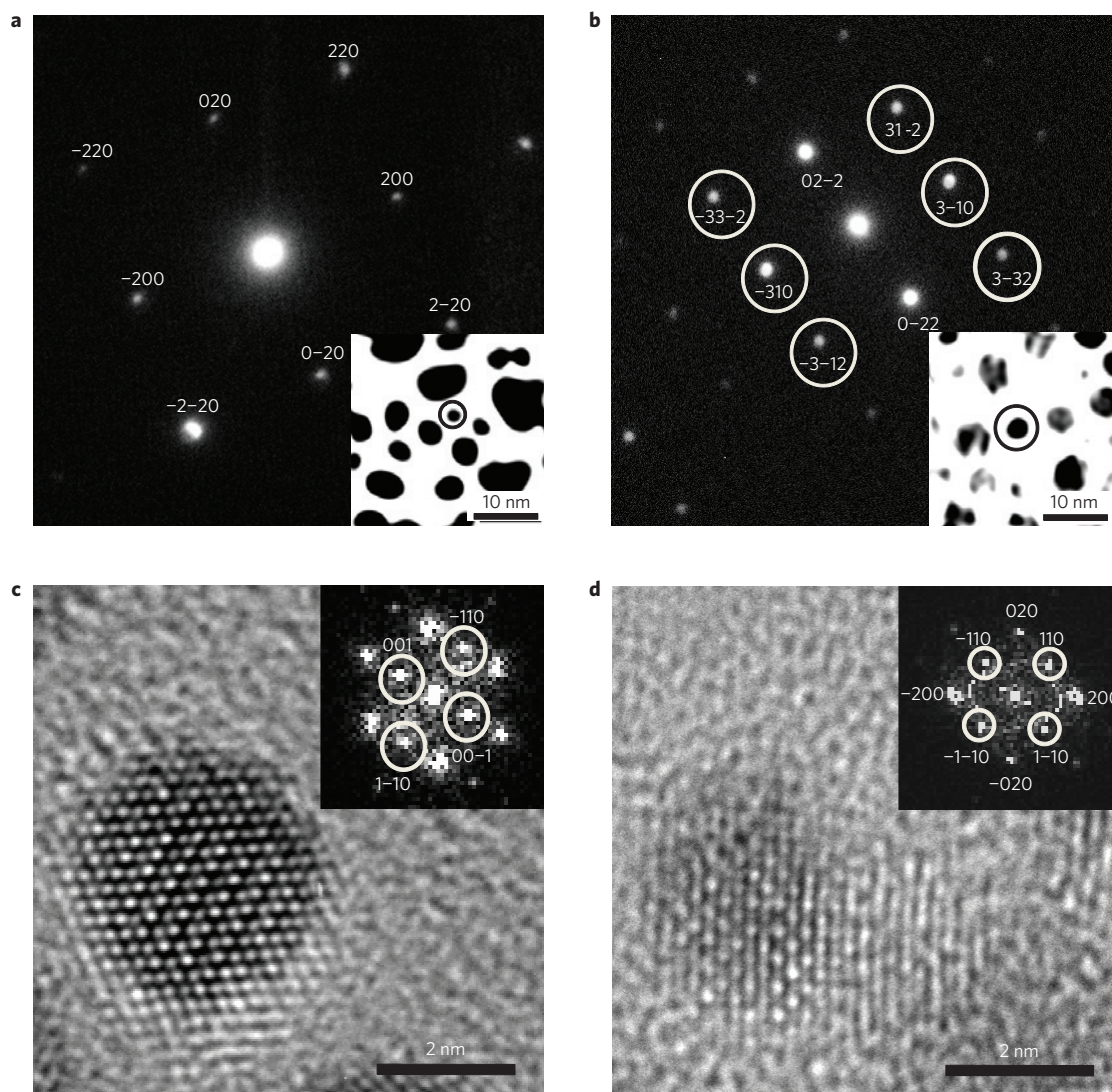
Figure 2 | Structural analysis by TEM: experimental evidence for the size effect. a, NBD pattern of a 2.4-nm-diameter disordered nanoparticle oriented along the [001] zone axis. **b**, NDB pattern of a 3.2-nm-diameter ordered nanoparticle oriented along the [133] zone axis (the superstructure reflections are circled). Insets of **a** and **b**: low-pass filtered TEM bright-field image showing the nanoparticle (circled) from which the NBD pattern was recorded. **c**, HREM image of a 3.8-nm-diameter ordered nanoparticle oriented along the [110] zone axis. Images **a–c** were acquired on the 1 nm nominal-thickness sample annealed at 750 °C. **d**, Ordered, 2.4-nm-diameter nanoparticle oriented along the [001] zone axis found in the 1 nm nominal-thickness specimen annealed at 500 °C for 16 h. The superstructure reflections are circled in the numerical Fourier transform of the image shown in the insets of **c** and **d**.

of the nanoparticles (Fig. 1, insets) evolve as a consequence of two processes, namely, coalescence and Ostwald ripening[25]. These growth mechanisms are thermally activated and their influence on the morphological parameters of the nanoparticles obviously depends on both temperature and annealing time. In an *in situ* heating experiment in a TEM reported in previous work[26], we have shown a rapid size increase of CoPt particles embedded in an alumina matrix when the temperature is above 700 °C. Accordingly, there was almost no evolution of the nanoparticle morphology in the samples annealed at 650 °C, whereas both the mean size and the polydispersity were significantly larger in the two samples after the annealing at 750 °C (Table 1).

Given the presence of polydispersity in the sample, it was necessary to use a local characterization tool to determine simultaneously the structure and the size of individual nanoparticles. This has been achieved by using transmission electron microscopy in high-resolution (HREM) and nanobeam-diffraction (NBD) modes. A nanoparticle is found in an ordered state if a set of superstructure reflections in the NBD pattern can be identified. Superstructure

reflections are not observed on the diffraction pattern of an ordered structure in a [*uvw*] zone axis orientation when *u* and *v* do not have the same parity and *w* is odd. Therefore, a nanoparticle is considered disordered if superstructure reflections are missing from its diffraction pattern in a particular zone axis orientation in which superstructure reflections would otherwise appear if the nanoparticle was ordered. Only a limited set of low-index zone axes could be used to unambiguously determine the disordered state of a nanoparticle. Given the random distribution of orientations of the nanoparticles, a large number of them must be probed to obtain a statistically significant set of nanoparticles in a suitable zone axis orientation. This could be done efficiently using the recently developed STEM/NBD (ref. 27) technique, which greatly improved the speed of the structural analysis of nanoparticles (see the Methods section). By combining the STEM mode imaging facilities of a TEM with a small (1 nm) parallel nanobeam, this new technique allows one to rapidly analyse a large number of nanoparticles, and to correlate the size of a nanoparticle with its state of order. The following results are based on the analysis of more than 100 particles on each sample.
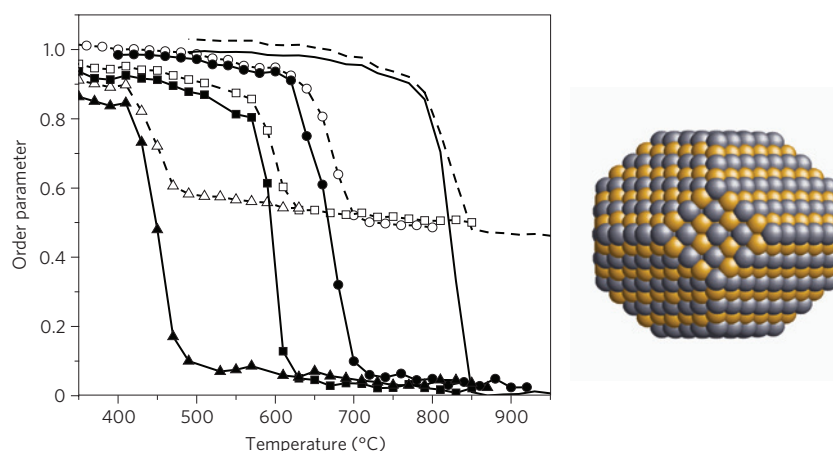
Figure 3 | Monte Carlo simulations: numerical evidence for the size effect. Order parameter for various temperatures calculated by Monte Carlo simulations of bulk CoPt (no symbol), a 3-nm-diameter isotropic truncated octahedra (circles) with 1,289 atoms (model shown on the right), 2.5 nm (squares) with 807 atoms and 2 nm (triangles) with 405 atoms. Filled symbols/solid lines represent the LRO and open symbols/dashed lines, the short-range order (SRO) parameters (see the Methods section for their definition). The order–disorder transition temperature is determined from the position of the main inflection point. Note that the order–disorder temperature transition, and thus the inflexion point, of the LRO and the SRO curves coincide.

As a result, the $L1_0$ phase was never observed in the 0.5 nm nominal-thickness samples, independently of the annealing temperature or the in-plane size of the nanoparticles. In the 1 nm nominal-thickness sample annealed at 650 °C, the nanoparticles were in the fcc disordered structure. For each sample, between 9 and 14 nanoparticles were found in a zone axis orientation, which confirmed their disordered structure without ambiguity. At 750 °C, nanoparticles with a mean diameter smaller than 3 nm are fcc disordered. Among the 34 analysed nanoparticles, three nanoparticles were found in a zone axis orientation showing without ambiguity the fcc structure, an example of which is shown by the NBD pattern of a 2.4-nm-diameter nanoparticle oriented along the ⟨001⟩ zone axis (Fig. 2a). The $L1_0$ ordered phase is observed in the sample with 1 nm nominal thickness annealed at 750 °C only for nanoparticles with a size larger than 3 nm. Among 75 analysed nanoparticles in this range of size, we did not find any nanoparticle in a zone axis orientation showing unambiguously the fcc structure. Figure 2b shows the NBD pattern from a 3.2-nm-diameter nanoparticle oriented along the [133] zone axis showing the 3–10, 3–32 and 31–2 superstructure reflections. On the HREM image of a 3.8-nm-diameter nanoparticle oriented along the [110] zone axis (Fig. 2c), the chemical order is evident from the difference in brightness between two successive planes of atoms along the [001] direction, which is directly related to the difference in the scattering factors of Co and Pt atoms. The ordering process in nanoparticles is a thermally activated kinetic process, which requires annealing conditions (time and temperature) to ensure sufficient atomic jumps occurring both at the surface and in the bulk of the nanoparticles. We have shown in previous work[26] that complete ordering occurs in CoPt nanoparticles with a mean size of 12 nm in less than 10 min in a temperature range of 650–750 °C. Consequently, the presence of fcc disordered structure of nanoparticles smaller than 3 nm, suggests that the phase transition occurs below 650 °C.

We have also carried out a series of 'virtual' experiments using canonical Monte Carlo simulations based on a many-body potential derived from the tight-binding model in the second moment approximation[28] (see the Methods section). The order parameter was calculated directly from the average atomic occupation of the lattice sites and was plotted at various temperatures (Fig. 3). The critical order–disorder temperature of a nanoparticle of a given size was then estimated from the inflexion point of this curve.

Indeed, these calculations show that the critical temperature of the order–disorder transition of the nanoparticles (T_C^{NP}) is shifted towards lower temperatures with decreasing cluster size[29]. For example, a 2.5-nm- and 3-nm-diameter particle have a T_C^{NP} 225 °C and 175 °C lower than T_C^{Bulk}, respectively (Fig. 3). For nanoparticles in this size range, the phase transition should thus occur between 600 and 650 °C (Fig. 3).

The simulations are consistent with the experimental observations according to which nanoparticles with a size smaller than 3 nm remain disordered when annealed at temperatures above 650 °C. The annealing temperatures used in the experiments are equal to or higher than the order–disorder transition of the nanoparticles, as estimated from the Monte Carlo simulations. This conclusion is in apparent conflict with the recent observations reported in ref. 30, according to which 2-nm-diameter CoPt nanoparticles were found ordered following a 2-h anneal at 650 °C. The mismatch could arise from the difference in the nature of the local environment (that is, substrate or protective layer), which is known to affect the thermodynamic stability of nanoparticles[31]. Indeed, we used amorphous alumina, whereas the nanoparticles analysed in ref. 30 were embedded in amorphous carbon.

No experimental study has precisely and quantitatively measured the size effect on the order–disorder transition. The experimental difficulty stems from the fact that annealing temperatures of these small particles must be carried out below T_C^{NP}, itself markedly lower than T_C^{Bulk}. Given that ordering is a thermally activated phenomenon[26,32], extended annealing times are required to induce ordering at lower temperatures, as is illustrated with the following experiment. We have annealed the 1 nm nominal-thickness sample at 500 °C for 16 h (which was previously annealed at 650 °C for 1 h). After this annealing process, we found chemically ordered particles in a range of size over 2.4 nm. Figure 2d shows a HREM image of an ordered CoPt nanoparticle with a size of 2.4 nm oriented along the [001] direction. This result demonstrates that the size effect, preventing the particle from ordering, can be overridden if the annealing temperature remains below T_C^{NP} and if the annealing time is sufficiently long for atomic diffusion to occur.

In striking agreement with our Monte Carlo investigation, we conclude that the T_C^{NP} of particles in the size range 2.4–3 nm, is between 500 and 650 °C. This work not only demonstrates experimentally the depression of the transition temperature with decreasing cluster size, as predicted by Monte Carlo simulations,
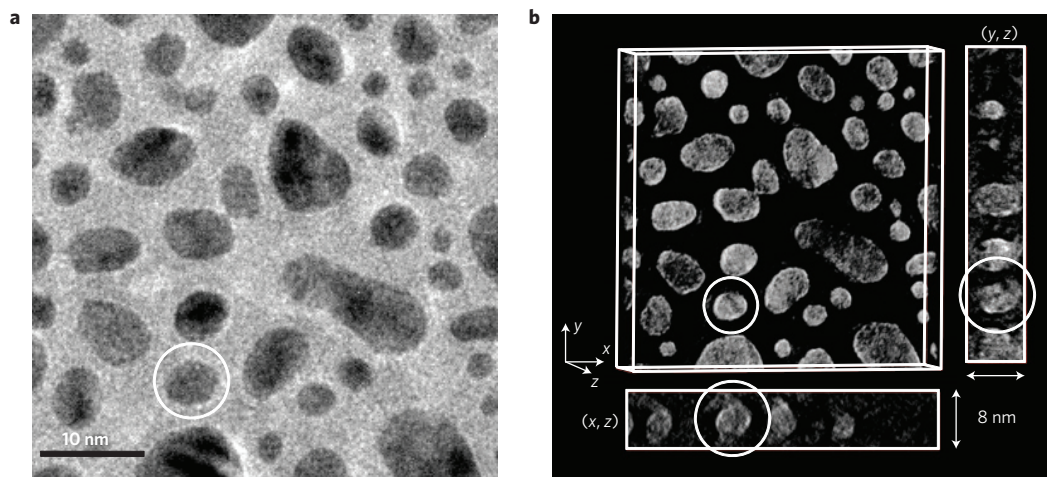
Figure 4 | 3D morphology of the particles. a, Bright-field image of the CoPt nanoparticles from the 1 nm nominal thickness sample annealed at 750 °C. **b**, Tomogram of the same area. The (x, z) and the (y, z) slices correspond respectively to the horizontal and vertical cross-sections of the tomogram. The 4 nm in-plane size nanoparticle circled in **a** and **b** has a thickness of 4 nm deduced from the slice images. This nanoparticle has an apparent thickness of 5.6 nm (average value of the measurements on the (x, z) and the (y, z) slices). Owing to the missing wedge, the tomogram is elongated along the z direction by a factor of 1.4 (see the Methods section).
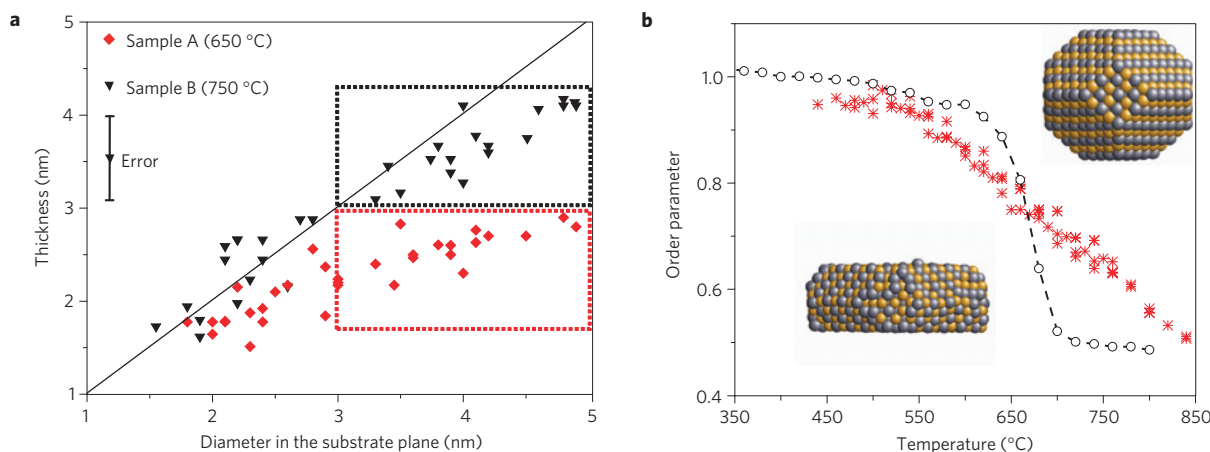

Figure 5 | Shape effect on the structural properties of CoPt nanoparticles. a, Correlation plot of the CoPt nanoparticles' thickness and their size in the plane of the substrate measured on the 1 nm nominal-thickness specimens annealed at 650 °C (red diamonds) and at 750 °C (black triangles). The black line corresponds to spherical particles. The dotted red and black rectangles enclose the data of the corresponding specimen in the 3–5 nm range of in-plane size. **b**, SRO parameter for various temperatures calculated by Monte Carlo simulations of an anisotropic truncated octahedron with 1.5 nm thickness and 4 nm in-plane width (stars, model illustrated in the bottom left) with 1,454 atoms, as compared with the isotropic 3 nm truncated octahedron (open circles, model illustrated in the top right).

but also demonstrates the possibility of controlling the ordering state of very small magnetic alloy particles.

There exists an overlap between the size distributions of the 1 nm nominal thickness sample annealed at 650 °C and the one annealed at 750 °C (subsequently referred to as sample A and sample B, respectively). According to the aforementioned observations, nanoparticles in the 3–5 nm range should be ordered. Although this is the case for nanoparticles in sample B, the nanoparticles in sample A were found to be surprisingly disordered. This mismatch clearly demonstrates that the nanoparticle size, as measured in the substrate plane, is not the only parameter affecting order–disorder phenomena in equiatomic CoPt nanoparticles.

To resolve this apparently conflicting result, we have investigated the nanoparticles' thickness as a function of their in-plane size by electron tomography. The basic principle of this technique is to reconstruct the three-dimensional (3D) morphology of the nanoparticles from a tilting series of 2D images of the nanoparticles (see the Methods section).

A bright-field image of a selected area in sample B is shown in Fig. 4a and the corresponding 3D representation (tomogram) is shown in Fig. 4b (see a 3D rotation of the tomogram in Supplementary Video). The morphology of each nanoparticle can be finely analysed by slicing the tomogram in the two perpendicular x and y directions. The thickness of the nanoparticles was deduced from the sliced images, corresponding to the (x, z) or the (y, z) planes[33]. As an example, the 4 nm in-plane size nanoparticle encircled on Fig. 4a,b has a thickness of 4 nm deduced from the sliced images.

The plot in Fig. 5a shows that the nanoparticles annealed at 650 °C have a nearly spherical shape only for in-plane sizes around 2 nm. However, nanoparticles annealed at 650 °C in the size range 3–5 nm (defined within the dotted red rectangle) are flatter than the ones annealed at 750 °C and their thickness is smaller than 3 nm. Alternatively, nanoparticles annealed at 750 °C have a thickness larger than 3 nm in the same range of size (dotted black rectangle in Fig. 5a). We can clearly observe that nanoparticles with a

nearly spherical shape are more abundant in specimen B. This spherical morphology indicates that a temperature of 750 °C is high enough to ensure the thickening of the nanoparticles by surface self-diffusion of Co and Pt atoms. We implicitly conclude that among the nanoparticles with an in-plane size larger than 3 nm, those with a thickness smaller than 3 nm (annealed at 650 °C) are always fcc disordered, whereas the nanoparticles with a thickness larger than 3 nm (annealed at 750 °C) are $L1_0$ ordered.

These results attest that only one dimension of a particle smaller than 3 nm is sufficient to induce a significant decrease of the order–disorder phase transition temperature, thereby inhibiting the particle ordering for annealing temperatures above T_C^{NP}. In other words, we have clear experimental evidence that the order–disorder transition temperature is not only sensitive to the size but also to the shape of the nanoparticles. This is the first time that the influence of the nanoparticles' shape on their structural properties is experimentally demonstrated.

The influence of morphology on the order–disorder transition is also consistent with the results of the Monte Carlo simulations of nanoparticles with a different aspect ratio. In Fig. 5b, we can observe that the theoretical order–disorder transition of anisotropic nanoparticles with dimensions close to the ones of the experimental particles (4 and 1.5 nm for the size and the thickness, respectively) is clearly shifted towards lower temperatures, compared with the bulk values. The transition point depression is almost identical to that of the isotropic particle of 3 nm and confirms the necessity of taking into account the aspect ratio of clusters to understand and control the order–disorder transition of bimetallic nanoparticles.

Laser-synthesized nanoparticles were annealed at various temperatures to study the physical parameters affecting the order–disorder transition. By using local characterization TEM techniques, we have correlated the size and the state of order of CoPt nanoparticles annealed at various temperatures. In striking agreement with our canonical Monte Carlo simulations, we could establish that 2.4–3-nm-diameter CoPt nanoparticles have a T_C^{NP} in the 500–650 °C range, which is 325–175 °C lower than the bulk transition temperature. For nanoparticles in this size range, we have demonstrated the possibility of inducing ordering albeit at a lower critical temperature, by compensating slower diffusion processes with extended annealing time. Moreover, using electron tomography, we have shown that the size effect on the critical temperature is uniquely determined by the smallest characteristic length of a nanoparticle. This phenomenon, also consistent with our Monte Carlo simulations, demonstrates that the aspect ratio, in addition to the observed size, affects the transition temperature of nano-objects. It is proposed that the concepts and the methodology proposed in this work to study size-induced phenomena be extended to and tested for various phase transformations or transitions occurring in nanoparticles.

Methods

Sample preparation. The CoPt nanoparticle thin films were produced by PLD in an ultrahigh vacuum chamber ($<10^{-7}$ mbar). This vapour phase deposition technique widely described in refs 26 and 31, was used to deposit alternatively cobalt and platinum by using a KrF excimer laser at 248 nm with a pulse duration of 25 ns at a repetition rate of 5 Hz. Commercial TEM Cu grids on which a 10-nm-thick amorphous carbon film was deposited were used as the substrate. Following the synthesis, the specimens were covered with a 2-nm-thick layer of amorphous Al_2O_3 deposited by PLD to protect the nanoparticles from air oxidation. Two samples, with 0.5 and 1 nm nominal thicknesses, were prepared at a substrate temperature of 25 °C and were subsequently annealed at 650 and 750 °C for 1 h. The samples were quenched to room temperature after annealing to avoid phase transformations during the cooling process.

TEM experiments. All of the TEM experiments were carried out on a JEM-2100F field-emission electron microscope operating at 200 kV and equipped with a high-resolution pole piece.

The STEM/NBD technique[27] is a method based on the use of the STEM mode imaging in a TEM with nearly parallel illumination conditions. Such conditions,

close to the ones used in NBD experiments, were obtained by adjusting the focal lengths of the microscope illumination lenses. With these adjustments, we were able to obtain a probe size of 1 nm and a convergence angle smaller than 1 mrad. The technique offered an accurate control of the beam position, which allowed us to obtain diffraction patterns of a large number of individual nanoparticles selected in the digital STEM image.

The data of the tomography experiments were acquired between −66° and +66° with 1° step increments by recording one image per tilt angle with a Gatan Slow Scan 2k × 2k camera. Between each tilt step, the lateral specimen shift and the objective focus were corrected manually. A 3D reconstruction was computed using a weighted back-projection algorithm, and the tomogram slicing was done with TEMography II, which is a system of TEM data series acquisition and a 3D-reconstruction package adapted for TEM developed by JEOL.

The methodology to determine the nanoparticle thickness on the tomogram has been described in ref. 33. The precision of measurements is equal to ±0.5 nm. The resolution of the tomogram was calculated to be equal to 0.9 nm, which indicates a good quality of the reconstruction mainly owing to a good signal/noise ratio.

The composition of the nanoparticles was measured using the JED-2300T energy-dispersive X-ray analyser from JEOL. To calibrate the X-ray analyser, we determined the Cliff–Lorimer k-factor[34] with a $Co_{45}Pt_{55}$ reference bulk sample. The bias in the k factor arising from the relative difference in the absorption behaviour of the Co K and Pt M X-ray lines was corrected using the procedure proposed in ref. 35.

Monte Carlo simulations using tight-binding potentials. The thermodynamics calculations consist of canonical Monte Carlo simulations using the Metropolis algorithm and many-body tight-binding potentials[28]. The parameters for the CoPt system were taken from ref. 29. In the canonical ensemble, Monte Carlo trials are of three kinds: random displacements of randomly chosen atoms, exchanges between two randomly chosen atoms of different species and in the case of the bulk, with periodic conditions, a box expansion in each direction. The order parameter is determined by statistical averaging as follows. The LRO parameter for the $L1_0$ phase is defined as the maximum value among the three directional order parameters $\eta_i = (p_A - 1/2) + (p_B - 1/2)$ with $i = x, y, z$, where p_A and p_B are the occupation probabilities on each sublattice of the $L1_0$ phase for the atoms of type A and B. This definition, as given in refs 28 and 29, assumes the possible fluctuations among the different variants of the $L1_0$ phase in small clusters. The short-range order (SRO) parameter, which becomes relevant in the case of finite systems, is defined by: $1 - (m - m_0/c_- m_0)$, where m and m_0 are the number of heterogeneous first-neighbour bonds in the system (in the $L1_0$ structure $m_0 = 8/12$) and c is the concentration. By definition, this parameter is equal to one in the ordered phase and zero in the disordered one. However, this parameter does not converge to zero after the transition, as seen in Fig. 3, because of residual short-range ordering, whereas the LRO parameter does. Nevertheless, we verified that the order–disorder transitions, as measured from the inflexion point of the SRO and LRO curves, are equivalent.

Finally, the absolute temperatures in Figs 3 and 5b have been shifted rigidly to fit the experimental bulk transition temperature, knowing that our model underestimates it by 180 °C.

References

1. Plumer, M. L., Van Ek, J. & Weller, D. *The Physics of Ultra-High-Density Magnetic Recording* (Springer, 2001).
2. Sellmyer, D. J., Yu, M. & Kirby, R. D. Nanostructured magnetic films for extremely high density recording. *Nanostruct. Mater.* **12,** 1021–1026 (1999).
3. Yu, M., Liu, Y. & Sellmyer, D. J. Nanostructure and magnetic properties of composite CoPt:C films for extremely high-density recording. *J. Appl. Phys.* **87,** 6959–6961 (2000).
4. Himpsel, F. J., Ortega, J. E., Mankey, G. J. & Willis, R. F. Magnetic nanostructures. *Adv. Phys.* **47,** 511–597 (1998).
5. Weller, D. & Moser, A. Thermal effect limits in ultrahigh-density magnetic recording. *IEEE Trans. Magn.* **35,** 4423–4439 (1999).
6. Ariake, J., Chiba, T., Watanabe, S., Honda, N. & Ouchi, K. Magnetic and structural properties of Co–Pt perpendicular recording media with large magnetic anisotropy. *J. Magn. Magn. Mater.* **287,** 229–233 (2005).
7. Klemmer, T., Hoydick, D., Okumura, H., Zhang, B. & Soffa, W. A. Magnetic hardening and coercivity mechanisms in L10 ordered FePd ferromagnets. *Scr. Metallurg. Mater.* **33,** 1793–1805 (1995).
8. Sakuma, A. First principle calculation of the magnetocrystalline anisotropy energy of FePt and CoPt ordered alloys. *J. Phys. Soc. Jpn* **63,** 3053–3058 (1994).
9. Christodoulides, J. A. *et al*. CoPt and FePt thin films for high density recording media. *J. Appl. Phys.* **87,** 6938–6940 (2000).
10. Sato, K., Bian, B. & Hirotsu, Y. Fabrication of oriented $L1_0$–FePt and FePd nanoparticles with large coercivity. *J. Appl. Phys.* **91,** 8516–8518 (2002).
11. Sato, K. & Hirotsu, Y. Magnetoanisotropy, long-range order parameter and thermal stability of isolated $L1_0$ FePt nanoparticles with mutual fixed orientation. *J. Magn. Magn. Mater.* **272–276,** 1497–1499 (2004).

12. Yasuda, H. & Mori, H. Effect of cluster size on the chemical ordering in nanometer-sized Au-75 at.%Cu alloy clusters. *Z. Für Phys. D* **37**, 181–186 (1996).
13. Miyazaki, T. *et al.* Size effect on the ordering of $L1_0$ FePt nanoparticles. *Phys. Rev. B* **72**, 144419 (2005).
14. Takahashi, Y. H., Ohkubo, T., Ohnuma, M. & Hono, K. Size effect on the ordering of FePt granular films. *J. Appl. Phys.* **93**, 7166–7168 (2003).
15. Sato, K., Hirotsu, Y., Mori, H., Wang, Z. & Hirayama, T. Long-range order parameter of single $L1_0$–FePd nanoparticle determined by nanobeam electron diffraction: Particle size dependence of the order parameter. *J. Appl. Phys.* **98**, 024308 (2005).
16. Yang, B., Asta, M., Mryasov, O. N., Klemmer, T. J. & Chantrell, R. W. The nature of A1–$L1_0$ ordering transitions in alloy nanoparticles: A Monte Carlo study. *Acta Mater.* **54**, 4201–4211 (2006).
17. Chepulskii, R. V. & Butler, W. H. Temperature and particle-size dependence of the equilibrium order parameter of FePt alloys. *Phys. Rev. B* **72**, 134205 (2005).
18. Muller, M. & Albe, K. Lattice Monte Carlo simulations of FePt nanoparticles: Influence of size, composition, and surface segregation on order–disorder phenomena. *Phys. Rev. B* **72**, 094203 (2005).
19. Moskovkin, P. *et al.* Model predictions and experimental characterization of Co–Pt alloy clusters. *Eur. Phys. J. D* **43**, 27–32 (2007).
20. Moskovkin, P. & Hou, M. Metropolis Monte Carlo predictions of free Co–Pt nanoclusters. *J. Alloys Compounds* **434–435**, 550–554 (2007).
21. Le Bouar, Y., Loiseau, A. & Finel, A. Origin of the complex wetting behaviour in Co–Pt alloys. *Phys. Rev. B* **68**, 224203 (2003).
22. Dai, Z. R., Sun, S. & Wang, Z. L. Phase transformation, coalescence, and twinning of monodisperse FePt nanocrystals. *Nano Lett.* **1**, 443–447 (2001).
23. Yu, A. C. C., Mizuno, M., Sasaki, Y., Kondo, H. & Hiraga, K. Structural characteristics and magnetic properties of chemically synthesized CoPt nanoparticles. *Appl. Phys. Lett.* **81**, 3768–3770 (2002).
24. Wang, A., Li, T., Zhou, Y., Jiang, H. & Zheng, W. Coupled Co–Pt nanoparticles in C matrix. *Mater. Sci Eng. B* **103**, 118–121 (2003).
25. Zinke-Allmang, M., Feldman, L. C. & Grabow, M. H. Clustering on surfaces. *Surf. Sci. Rep.* **16**, 377–463 (1992).
26. Alloyeau, D., Langlois, C., Ricolleau, C., Le Bouar, Y. & Loiseau, A. A TEM *in situ* experiment as a guideline for the synthesis of as-grown ordered CoPt nanoparticles. *Nanotechnology* **18**, 375301 (2007).
27. Alloyeau, D. *et al.* STEM nanodiffraction technique for structural analysis of CoPt nanoparticles. *Ultramicroscopy* **108**, 656–662 (2008).
28. Rosato, V., Guillopé, M. & Legrand, B. Thermodynamical and structural properties of fcc transition metals using a simple tight-binding model. *Phil. Mag. A* **59**, 321–336 (1989).
29. Rossi, G., Ferrando, R. & Mottet, C. Structure and chemical ordering in CoPt nanoalloys. *Faraday Discuss.* **138**, 193–210 (2008).
30. Tournus, F. *et al.* Evidence of $L1_0$ chemical order in CoPt nanoclusters: Direct observation and magnetic signature. *Phys. Rev. B* **77**, 144411 (2008).
31. Langlois, C. *et al.* Growth and structural properties of CuAg and CoPt bimetallic nanoparticles. *Faraday Discuss.* **138**, 375–391 (2008).
32. Rellinghaus, B. *et al.* On the $L1_0$ ordering kinetics in Fe–Pt nanoparticles. *IEEE Trans. Magn.* **42**, 3048 (2006).
33. Alloyeau, D. *et al.* Comparing electron tomography and HRTEM slicing methods as tools to measure the thickness of nanoparticles. *Ultramicroscopy* **109**, 788–796 (2009).
34. Cliff, G. & Lorimer, G. W. The quantitative analysis of thin specimen. *J. Microsc.* **1032**, 203–207 (1975).
35. Van Cappellen, E. The parameterless correction method in X-ray microanalysis. *Microsc. Microanal. Microstruct.* **1**, 1–22 (1990).

Acknowledgements

Author contributions

D.A. prepared the samples. D.A., C.R. and T.O. developed the STEM/NBD technique and carried out the TEM experiments. D.A. analysed the experimental data. C.M. carried out the Monte Carlo simulations and described them in the article. C.R., Y.L.B., C.L. and A.L. supervised the project. D.A. and C.R. prepared the manuscript. N.B. contributed to the energy-dispersive X-ray data analysis and improved the writing of the article. All authors discussed the results and implications and commented on the manuscript at all stages.

Additional information